Wiley
International Transactions on Electrical Energy Systems
Volume 2024, Article ID 3353622, 19 pages
https://doi.org/10.1155/2024/3353622

WILEY

Research Article

Distribution System Operator (DSO) Functions in South Korea—Part I: Development, Practical Obstacles, and Future Work

Jung-Sung Park,[1] Jun-Hyeok Kim,[2] Seung-Gil Noh,[2] Woo-Young Cho,[2] Han-Kyul Kim,[2] Balho H. Kim,[3] and Yun-Su Kim [2]

[1]*Smart Power Distribution Lab, KEPCO Research Institute, Daejon 34056, Republic of Korea*
[2]*Graduate School of Energy Convergence, Gwangju Institute of Science and Technology, Gwangju 61005, Republic of Korea*
[3]*Department of Electronic and Electrical Engineering, Hongik University, Seoul 04066, Republic of Korea*

Correspondence should be addressed to Yun-Su Kim; yunsukim@gist.ac.kr

Received 26 September 2023; Revised 2 October 2024; Accepted 17 October 2024

Academic Editor: Hamed Badihi

This paper presents our initial research findings on distribution system operator (DSO) functions in South Korea. The project team includes the Korean Electric Power Corporation, which is the only public utility company in South Korea. The planned development is based on a real distribution network and real-world environments. The project encompasses DSO–transmission system operator coordination and management of real-time distribution network congestion; this paper focuses on the latter aspect. For real-time congestion management, algorithms that handle all steps from database analysis to data export, including data preprocessing, topological configuration, power flow calculation, sensitivity analysis, and derivation of solutions to congestion, are developed. The distribution system equipment database of Korean Electric Power Corporation is used to develop a network congestion management system. When examining the database, many gaps between the theoretical and practical environments were found which are introduced in this paper. A practical distribution network database for South Korea is developed to narrow these gaps and to implement practical congestion management techniques. The remaining problems are introduced as future works.

1. Introduction

In November 2016, the South Korean government permitted unrestricted interconnection of small-scale (≤ 1 MW) distributed energy resources (DERs) within the distribution network [1]. Technically, unrestricted interconnection with a grid is impossible, but the only Korean public utility provider and distribution network owner (DNO), i.e., the Korean Electric Power Corporation (KEPCO), was requested to host as many DERs as possible. The installed DER capacity increased greatly from 6.9 GW at the end of 2016 to 17.4 GW at the end of 2020 [2]. Most DERs are renewable energy sources (RESs); their combined capacity (17.4 GW) is much larger than that of the transmission network (4.7 GW) [2]. However, according to the Tenth Basic Plan for South Korean Electricity Supply and Demand, 71.5 GW of RESs should be installed by 2030 [3].

Given the increases in the number of RESs, the transmission system operator (TSO), i.e., the Korean Power Exchange (KPX), has curtailed their power. For Jeju Island, which has the highest RES penetration of any South Korean region, wind turbine power was curtailed three times (total of 152 MWh) in 2015 (the first year of curtailments). In 2022, the number of curtailments increased dramatically to 93, and the total energy curtailment was 23,989 MWh. Photovoltaic (PV) power was curtailed only once (a total of 29 MWh) in 2021 (the first year of curtailments) in Jeju Island but was curtailed 28 times (a total of 3218.7 MWh) in 2022. As the

capacity of RESs in the distribution network is much larger than in the transmission network, the TSO (the KPX) must curtail power from the distribution network. However, the TSO lacks distribution network information, and KEPCO is not authorized to curtail or dispatch power from DERs. To solve this problem, a distribution system operator (DSO) that monitors the distribution network and is authorized to dispatch DERs is required; a research project aiming to achieve this commenced in 2020.

DSO definitions and roles have changed [4–7], and DSO functions may differ by country and utility type. In this paper, two DSO functions, i.e., distribution network analysis and the authority to dispatch DERs, are considered. These functions are usually performed by DER management systems (DERMSs) in other countries. In [5], the effects on a distribution system of a DSO using a DERM were analyzed. A South Korean DERMS (KDERMS) has been developed and is used by KEPCO to manage DERs. However, KEPCO still cannot use KDERMS for direct control of DERs because it lacks the authority. In [8], the Korean smart distribution management system (KSDMS) was presented and discussed in terms of the system architecture, data communication, and a common database (DB). The authors comprehensively described the key features of distribution network control, operation, and data processing. However, network congestion caused by the intermittent nature of RES power was not considered; congestion was not an issue at that time. Distribution network congestion was considered in [9–19]. In [9], electric vehicles (EVs) were used to prevent congestion; however, the authors conceded that distribution network analysis using a DSO is difficult. In [10], the effects of regulations on DER integration by the DSO were considered. However, DER control by a DSO was not discussed. A novel, optimal power flow technique was presented in [11]. Power flow management was automated to handle the thermal constraints of distribution networks. A calculated generator control signal was used to determine whether DERs should or should not be curtailed. In [12], a dynamic tariff subsidy method was developed for the management of congestion in distribution networks with high penetration for PVs, heat pumps, and EVs. In [13], an energy flexibility model allowed DSOs to provide day-ahead energy market prices without congestion. A swap method was proposed in [14] to manage real-time congestion in a distribution network. A distributed, optimization-based dynamic tariff method was proposed in [15] to manage congestion in distribution networks. In [16], resources in a distribution network are used for a transmission network operation. The distribution network congestion is checked if the power delivery from the resources to the transmission network is available without any congestion. In [17], a DSO platform framework is presented. A mixed-integer optimization model is formulated to manage flexibility services and congestion issues in a distribution network. The DSO platform framework is for Spanish project demonstration as the similar project for the Korean distribution network has been conducted. In [18], the amount of flexibility acquired from the distribution network is assessed considering the distribution network congestion. This work focuses on the assessment of the flexibility without congestion violation whereas our work focuses on the solution of the congestion if it happens in real time. So, the purpose of the work is different. In [19], the assessment of grid tariff designs for DSOs of some countries was performed. During the assessment, the distribution network congestions are considered since they affect the tariff. The summary of the comparison between DSO-related studies is shown in Table 1.

Studies that considered distribution network congestion [9–19] underestimated the network data acquisition requirement, which poses a practical problem. Most models used virtual test feeders with all network data. However, in practice, theoretical methods cannot be directly applied to a distribution network without consideration of the network DB. Based on our investigation of the Korean distribution network DB, it is found that the data structure and terminologies are focused on the maintenance of assets and equipment for field engineers. These are not suitable for the network analysis. For instance, phases are unidentified, which makes power flow calculation inaccurate. Furthermore, there are so many missing or damaged data. Sometimes, there are redundant data for the network analysis. For instance, in the DB, there are so much data regarding switches and two or more switches can be gathered at one node, but in terms of the network analysis, they can be simplified as a single node. Most theoretical analyses of power systems assess transmission networks, the data acquisition and information systems of which are of higher quality than those of distribution networks. For example, the transmission management system of South Korea acquires data every 2 s, whereas the distribution management system acquires data only every 15 min. When discussing the functions of the South Korean DSO, the following salient features of the distribution network must be kept in mind:

- South Korea has only one public DNO (KEPCO) and yet has no authorized DSO. Here, the terminology DSO is used as an operator who has the authority to adjust the output power of DERs in the distribution network whereas the DNO has not.
- KEPCO is also the sole retailer.
- KEPCO uses in-house DMSs and DERMs rather than commercial systems; the in-house models reflect the features of the Korean distribution network. Thus, DSO management of DERs must take account of this.
- Distribution network data are not integrated into a single management system for legal reasons (e.g., personal privacy). This renders distribution network analysis very difficult.

In this paper, some details of the DB of the Korean distribution network are discussed; these are important for distribution network analysis. Based on a real DB, topological configuration, calculated power flow, generated a sensitivity matrix, and managed possible congestion using DERs are developed. The existing methodologies are adopted for those analyses and calculations so this paper may not be able to take credit in terms of theoretical developments or improvements. However, this paper focuses on (1) sharing our experiences encountered while applying the existing theories to the real distribution network and (2)

Table 1: Comparison between what DSO-related studies considered.

Ref. No.	DER control	Congestion (real time)	Data structure	DSO-oriented solution	Real distribution network
[5]	V	X	X	V	V
[9, 16]	V	Δ	X	X	X
[10]	X	Δ	X	X	X
[11, 18]	V	Δ	X	V	V
[12]	X	Δ	X	V	X
[13, 15, 19–21]	V	Δ	X	V	X
[14]	V	V	X	V	X
[17]	V	Δ	X	X	V
Proposed work	V	V	V	V	V

Note: V: considered, X: not considered, Δ: congestion is considered but not real time.

the detailed procedures of the data processing and the algorithm developments. Yet, many tasks remain for subsequent research projects; these are also discussed. The contributions of this paper are as follows:

- The features and data of the South Korean distribution network are carefully explained which is very helpful for power systems engineers and scholars who lack practical information about distribution network operation.
- Practical obstacles encountered during distribution network analysis are illustrated in detail to narrow the gap between theory and practice.
- Management of congestion by controlling DERs is applied to a distribution network based on real data.
- Many future practical problems are illustrated in the hope that readers may be able to solve them.

The improvements due to the methods and algorithms proposed in this paper may not be proved quantitatively or analytically but they make the existing methods—e.g., power flow calculation and sensitivity analysis—being able to be adopted for future DSOs in Korea. The proposed algorithms cannot be mathematically optimized since there are no such metrics to measure the performance of those kinds of algorithms. Nevertheless, due to the usefulness and practicability of the proposed algorithms, it is expected that the proposed algorithms will become an essential part of the DSO function.

The rest of the paper is organized as follows: Section 2 briefly describes the entire system architecture of a real-time DSO, Section 3 discusses the topological configuration and details of the distribution network DB, Section 4 presents a congestion management technique involving load estimation and a sensitivity matrix, Section 5 shows the simulation results, and Section 6 discusses future tasks that must be completed before a real-time DSO can function perfectly.

2. System Architecture of a DSO Operating in Real Time

In this paper, "real time" indicates a 15-min time interval, which is relatively short compared to the previously used 1-h interval. This 15-min time interval accords with that of the Korean real-time power market currently under development. As described in Section 6, the time interval should be further reduced to exploit the agility of DERs.

Figure 1 illustrates the system architecture and data flow for the real-time DSO. It shows how each entity exchanges data with the other. The entities include real DERs, a commercial virtual power plant (CVPP), a DER emulator, field components, and a DSO. The DSO entity is illustrated in detail including the DB and the real-time DMS algorithm. The dataset matrices are in bold uppercase font and represent combinations of float, integer, and string data. Most datasets were derived from the KEPCO DB using the KEPCO algorithms. KEPCO is the DNO in Korea, but in this study, it is assumed that KEPCO is the DSO. Part of the real-time DMS algorithm was developed by the Power Systems Laboratory of the Gwangju Institute of Science and Technology. The DMS algorithm is used to manage congestion by applying the required curtailments to the DERs of an aggregator. Both voltage and line capacity violations are considered to reflect congestion, which is monitored by the distribution line (DL, also known as the main feeder); each DL is associated with datasets such as those shown in Figure 1. Real measurements from DERs, i.e., $\mathbf{M}^{\mathrm{rD}}$, are delivered to both the DSO and aggregator, which is a CVPP, via the smart gateway (SMGW). As the capacity to host a DER is regulated conservatively under the existing rules, the hosting capacity of the real distribution network is too low to cause congestion. Thus, DER emulators and virtual DERs (vDERs) have been used to interact with the CVPP and DSO, deliver $\mathbf{M}^{\mathrm{vD}}$ to the CVPP and DSO, and emulate congestion of the distribution network. The measurements obtained by feeder remote terminal units (FRTUs), i.e., $\mathbf{M}^{\mathrm{F}}$, are also delivered to the DSO. The measurement data of all real and vDERs, i.e., $\mathbf{M}^{\mathrm{D}}$, are the combination of $\mathbf{M}^{\mathrm{rD}}$ and $\mathbf{M}^{\mathrm{vD}}$. The major components of $\mathbf{M}^{\mathrm{D}}$ and $\mathbf{M}^{\mathrm{F}}$ are as follows:

- Timestamps: inputs of integral data.
- DLID: DL identification (ID) numbers of the DERs and the FRTUs (integral data).
- CEQID: conducting equipment (CEQ) ID numbers of the SMGWs of the various DERs for $\mathbf{M}^{\mathrm{D}}$ and FRTUs for $\mathbf{M}^{\mathrm{F}}$ (integral data).
- Three-phase active and reactive powers (per unit float data).

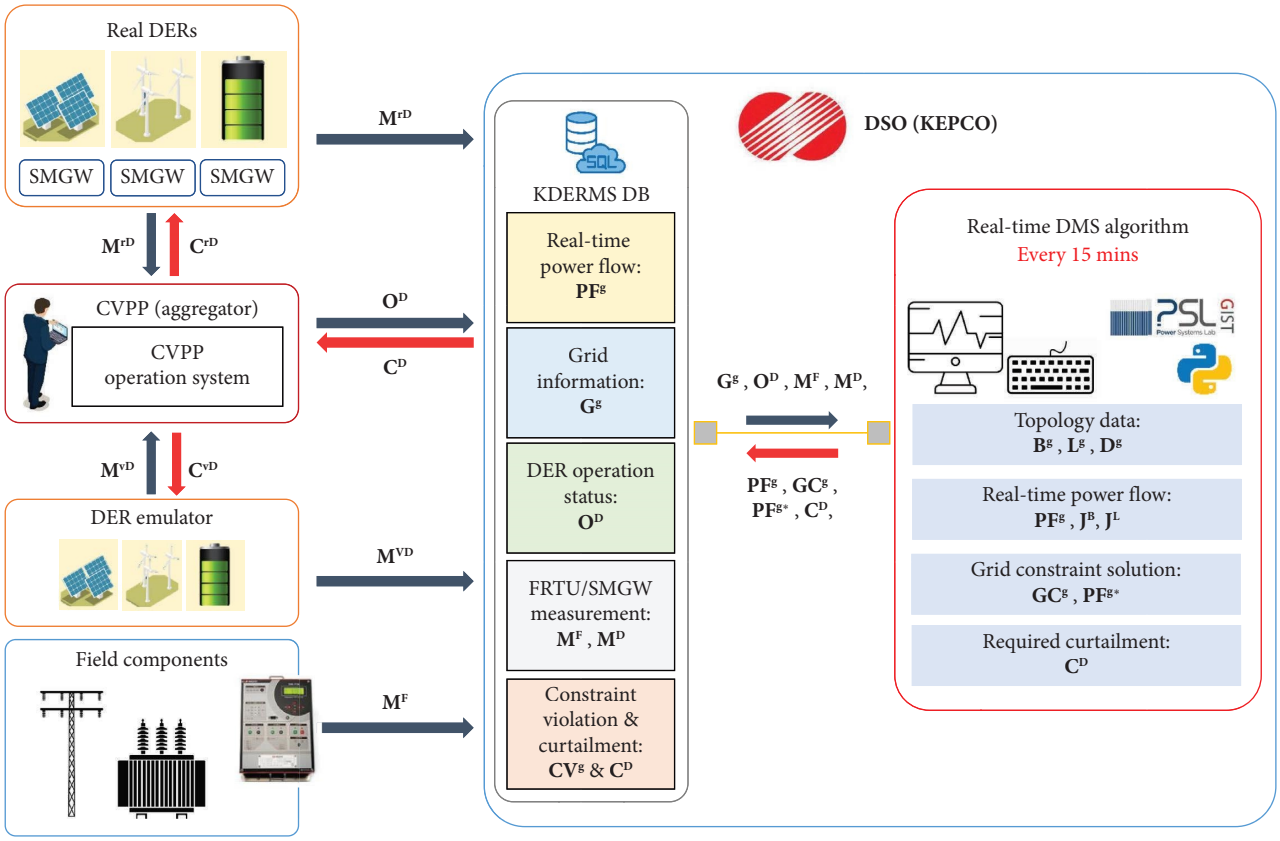

Figure 1: System architecture and data flow of a DSO operating in real time.

CEQs, such as switches and lines, are the basic constituents of the KDERMS DB. Terminals (Ts) and connectivity nodes (CNs) represent all connections among equipment in the KDERMS DB, as shown in Figure 2. As shown in Figure 2, CN connects every equipment, and T is generated at every point of equipment where it is connected to CN. Pad-mounted switches (PMSs), lines, and buses are the example of CEQs.

The KDERM DB is used for real-time congestion management of the distribution network and contains the grid information $\mathbf{G}^g$ and real-time operational information of the DERs ($\mathbf{O}^D$). The $\mathbf{G}^g$ includes information on connections between equipment using the Ts, CNs, and CEQID data of Figure 2. The major components of $\mathbf{O}^D$ are as follows:

- DerCode: DER code number (integral data).
- The DLIDs for the DERs (integral data).
- activePowerControllable denotes whether the DER active power is controllable (Boolean data; take a value of "1" if controllable and "0" if not controllable).
- downward/upwardControlAmount: the available downward/upward power to be controlled. Float data in per unit (pu).

The datasets shown in Figure 1 include a considerable amount of information, but only data that are relevant to this study are discussed for the sake of concision. The real-time DMS algorithm uses the KDERMS DB to generate the network topology to calculate power flow by checking network congestion in advance and to calculate the power curtailment required for each DER $\mathbf{C}^D$; this eliminates congestion. $\mathbf{C}^D$ is calculated for each DL and delivered to the KDERMS, CVPPs, and DERs (in that order), as shown in Figure 1.

Calculation of $\mathbf{C}^D$ is the main objective. A flowchart of the algorithm is shown in Figure 3; the algorithm starts by setting the system parameters, which are mainly the DER specifications. Then, the operator inputs (writes) the name of the DL to the algorithm, and the algorithm then imports the data of that DL from the DM of the KDERMS. When using the KDERMS DB, the topology configuration function generates a new network topology that can be used for power flow calculation. This is because the network topology and load information directly fetched from the KDERMS DB cannot be used for the power flow calculation. The topology and its data structure should be reorganized so that it can be used for the power flow calculation. More specifically, in the absence of a topological configuration, power flow calculation is impossible because the connectivity between devices is too complex, and some parts of the network are treated as unconnected; the number of nodes is excessive; and there is no load bus information. When using general power flow calculation methods, the load buses must be defined, but the KDERMs DB provides only the section loads, i.e., the load

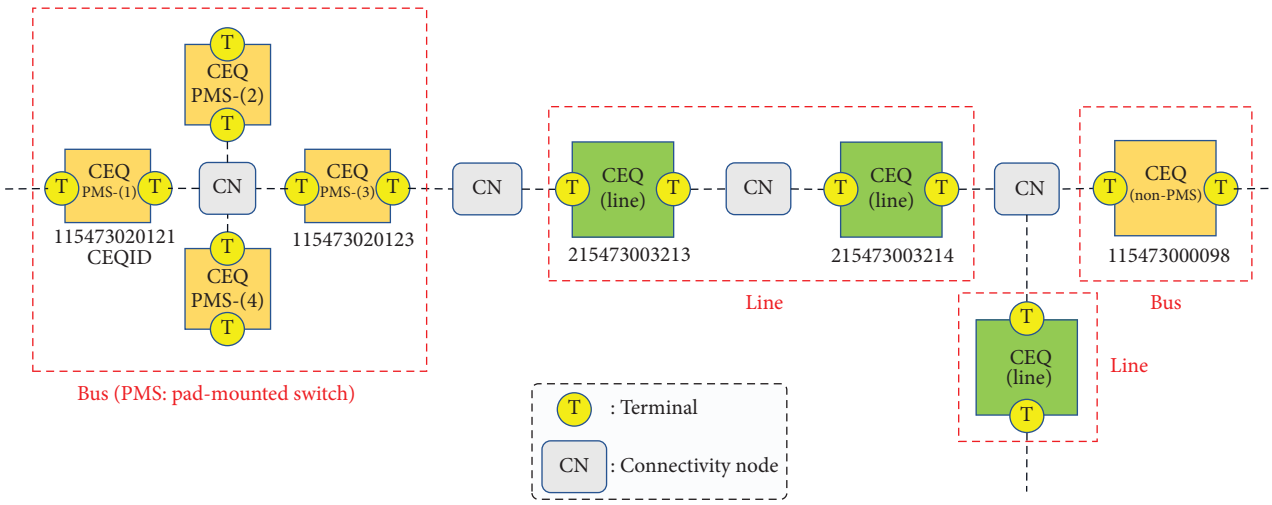

Figure 2: Schematic of the connections between CEQs.

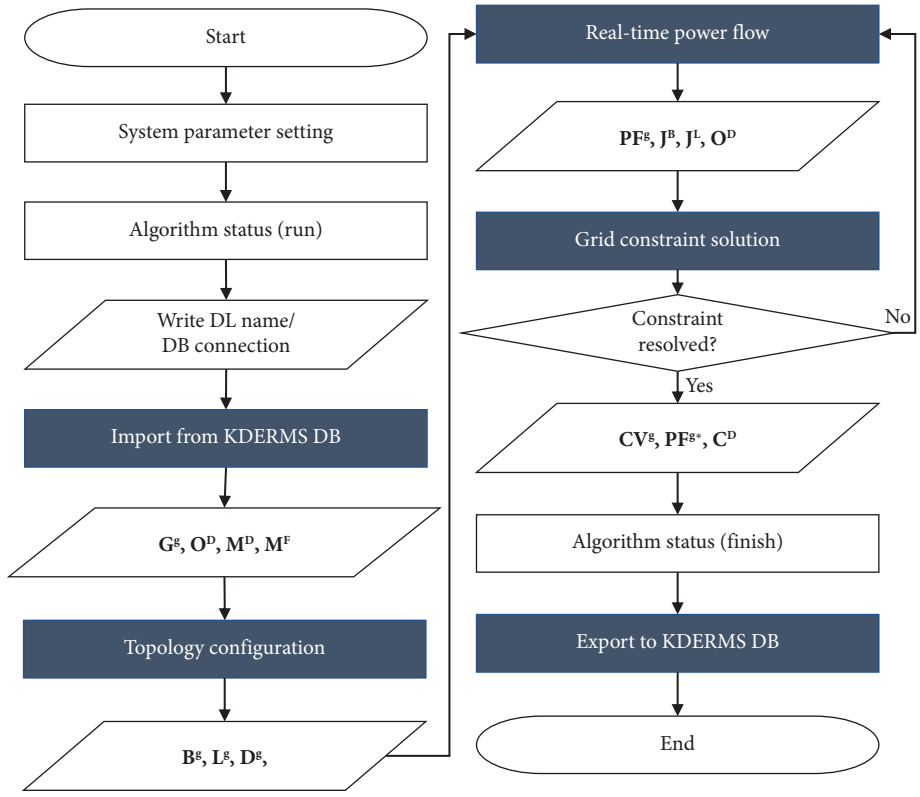

Figure 3: Flowchart of the real-time DMS algorithm.

consumptions between two consecutive FRTUs. Over these distances, and within single sections, there are usually more than two distribution transformers, each of which should be regarded as a load bus during general power flow calculation. However, as data on distribution transformers are usually unavailable, they must be treated as lumped loads at specific positions (nodes or buses); the details are discussed in Section 3. The new topology generates the bus, line, and DER configuration datasets ($\mathbf{B}^{g}$, $\mathbf{L}^{g}$, and $\mathbf{D}^{g}$, respectively). The $\mathbf{B}^{g}$ contains data for the CEQIDs, CEQ types, measured/calculated active and reactive powers, voltage magnitudes and phases, bus names, and bus types (slack, load, or generation).

$\mathbf{L}^{g}$ contains the data sent from/to the CEQIDs, as well as the resistances, reactance, and ampacities. $\mathbf{D}^{g}$ contains the names of the CVPPs and CEQIDs to which each DER belongs, as well as the efficiencies (of batteries), capacities, power ratings, and power generation data; the remaining information is analogous to that of $\mathbf{O}^{D}$.

The new topology is used for power flow calculation. The calculation function generates the power flow calculation results PF^{g}, Jacobian matrices $\mathbf{J}^{B}$ with respect to the bus injection powers, $\mathbf{J}^{L}$ with respect to the line flows, and DER operation status $\mathbf{O}^{D}$, which is updated on power flow calculation. These datasets are input to the grid constraint solution function, which then generated the constraint violations CV^{g}, revised power flows PF^{g*} that handle the violations, and required power curtailments $\mathbf{C}^{D}$ for all DERs.

3. Topology Configuration Module

One of the salient features of the KEPCO distribution network management is that they use their own management system developed by themselves unlike other utilities who use commercial software. The KEPCO has developed their own DB and their own way to process the data. One of the critical data processes is the topology configuration, which processes raw data in the DB into manageable data structure so that they can be handled easily by the existing network analysis methods—e.g., power flow calculation. So, to the best of our knowledge, there are no published works which describe the KEPCO distribution network topology configuration in details even though it is very critical process for the practical application of the existing methodologies. There is no generalized way to develop the topology configuration algorithm so this section is dedicated to describe the development process.

To import data from the KDERMS DB, a read input data module is developed, the flowchart of which is shown in Figure 4; the yellow box denotes the function of the module, the gray boxes constitute a data table, the blue box a set of data tables, and the orange box is another module. The read input data module collects KDERMS SQL server information by running the "readUserInfo," "connectPythontoSql," and "importSql" functions, as shown in Figure 4. The data are categorized as either static or dynamic. The corresponding DL data are saved in the dbTable, which contains ConductingEquipment, IdentifiedObject, Ts, PSRType, SectionParentView, and RealSwitchDataView data tables; these serve as inputs to the topology configuration module as shown in Figure 5.

The topology configuration module comprises five major functions: "ComposeTopology," "PreprocessTopology," "MakeRadial," "ReduceMeteredOnlyTopology," and "ImportMeteredData." The "ComposeTopology" function returns lists of the types of switches and CNs, identifies whether CNs are at the ends of lines or junctions between lines, whether or not a switch is multiterminal ("PMS" in Figure 2), and whether a switch is open or closed. The pseudocode for "ComposeTopology" is shown in Algorithm 1.

The "PreprocessTopology" function uses the output of the "ComposeTopology" function to return the initial reduced bus and line data tables $\mathbf{B}^{0}$ and $\mathbf{L}^{0}$, respectively. The tables contain the CEQIDs, Ts, CRQ names and types, line lengths, and impedances. The "ComposeTopology" function reduces the number of lines. For example, if three lines are consecutively connected without any intervening devices, they are reduced to a single line of equivalent impedance. The function also deletes de-energized buses and lines in the "Open Section." A topological change made using the "PreprocessTopology" function is shown in Figure 6, and the pseudocode is shown in Algorithm 2. As shown in Figure 6, the number of buses is decreasing as the multiterminal switches are replaced by a single switch and as open sections are deleted.

However, the numbers of buses and lines remain too large for power flow calculations. Thus, the "MakeRadial" and "ReduceMeteredOnlyTopology" functions are used to further reduce the network topology. The pseudocodes are shown in Algorithms 3 and 4, respectively.

Algorithm 3 accepts the initial line data table $\mathbf{L^0}$ and the index for the current line c as inputs, where n is the index for the next line, $\mathbf{L}_{cn}$ is the set of next lines of line c (l_c), and b_{lfd} and b_{ltd} are "from" the bus (l_d) and "to" the bus (l_d), respectively. The next line is the line connected to the "to" bus of the current line, which becomes the "from" bus of the next line. The algorithm rearranges the "from" bus and "to" bus information of each line assigning "from" buses to nodes upstream of both ends of a line and "to" buses to downstream nodes. The algorithm ends when there is no further line.

Algorithm 4 accepts $\mathbf{L^0}$ and $\mathbf{B^0}$ as inputs and returns updated $\mathbf{L^0}$ and $\mathbf{B^0}$ values, i.e., reduced topological information, where subscripts s and p denote a slack line (a line connected to a slack bus) and the previous line, respectively. **Stack** denotes the stack of data (here, the indices of the lines), and **Stack.push**(c) and **Stack.pop**() insert index c into the stack and erase the last index from the stack, respectively. The square brackets denote the "if" statement of the code for the sake of simplicity. The algorithm erases all buses except measurement buses $\mathbf{B}^{m}$ and junction buses $\mathbf{B}^{j}$, because the other buses are not required for network analysis. All lines sharing such buses are combined into a single line.

Finally, the updated $\mathbf{L^0}$ and $\mathbf{B^0}$ enter "ImportMeteredData," which returns $\mathbf{B}^{g}$, $\mathbf{L}^{g}$, and $\mathbf{D}^{g}$ as outputs. The major roles of this function are the importation of measured data and generation of load buses. For $\mathbf{B}^{m}$, only the power flows through lines are measured/acquired; there are no load buses in the data table at this time. To generate the load buses, the power flow measurements at either end of a section are subtracted; this yields the section load, which is then divided into a number of buses within the section (including T buses); the load is equally divided between all buses in the section. Data tables $\mathbf{B}^{g}$, $\mathbf{L}^{g}$, and $\mathbf{D}^{g}$ are shown in Tables 2, 3, and 4 where the names of data are written as generated in the codes.

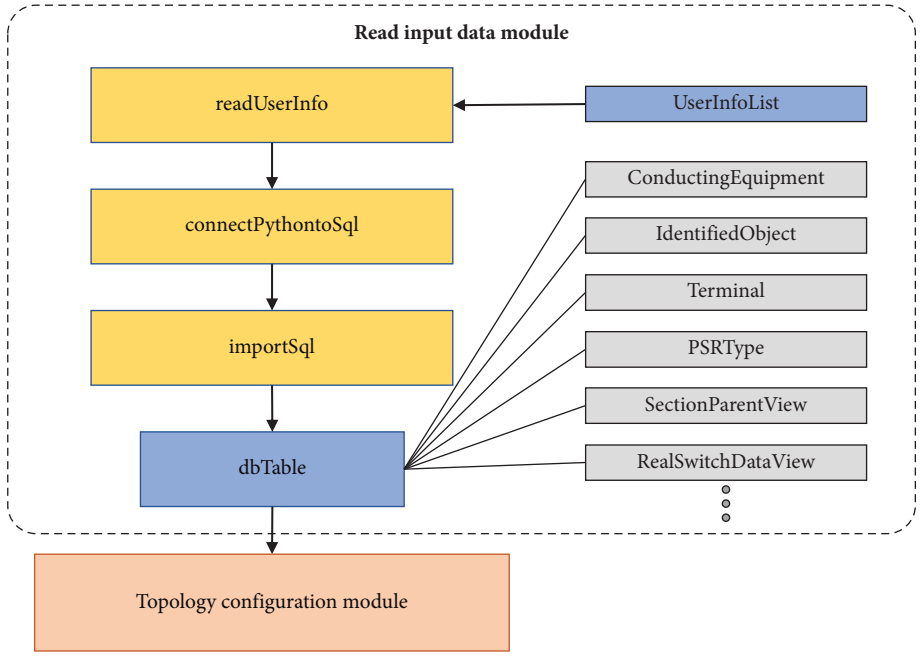

Figure 4: Flowchart of the read input data module.

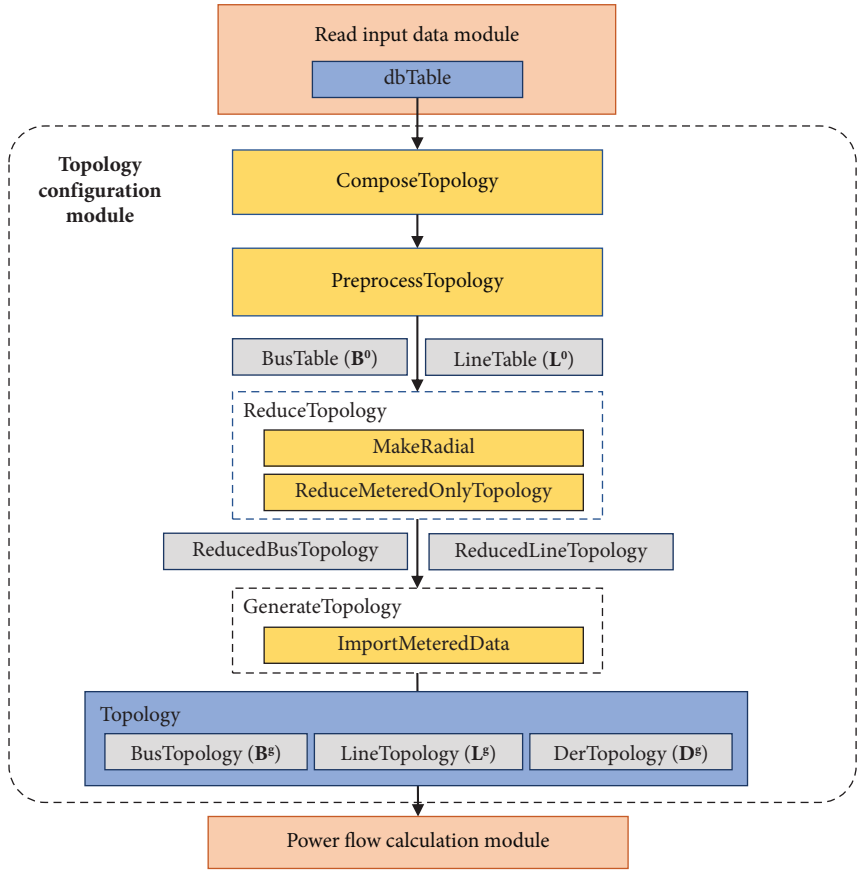

Figure 5: Flowchart of the topology configuration module.

Input: **CEQ**, **CN**
Output: $\mathbf{B^0}$, $\mathbf{L^0}$, PMS, $\boldsymbol{J}$, $\mathbf{L^{open}}$

1. if $\mathbf{CEQ}_k$ is bus then
2. $\mathbf{B^0}$ = **CEQ**[**CEQ**["type"] = = bus]
3. $\mathbf{L^0}$ = **CEQ**[**CEQ**["type"] = = line]
4. if $\mathbf{CN}_n$.terminal = $\mathbf{CEQ}_k$.terminal then ◄ count # of CN's connected CEQ
5. $\mathbf{CN}_n$ [count] ⟵ $\mathbf{CN}_n$ [count] + 1
6. if $\mathbf{CN}_n$ [count] = 1 then
7. delete [$\mathbf{L^0}$ connected to $\mathbf{CN}_n$ [count]]
8. if $\mathbf{CN}_n$ [count] = 2 then
9. generate [From-To info between **CEQ**]
10. if $\mathbf{CN}_n$ [count] = 3 then
11. add $\mathbf{CN}_n$ into $\boldsymbol{J}$
12. if $\mathbf{CN}_n$ [count] = 4 then
13. add ($\mathbf{CN}_n$) into PMS
14. delete $\mathbf{B^0}$ connected to $\mathbf{CN}_n$ [count]
15. add ($\mathbf{CN}_n$) into $\mathbf{B^0}$

Algorithm 1: ComposeTopology.

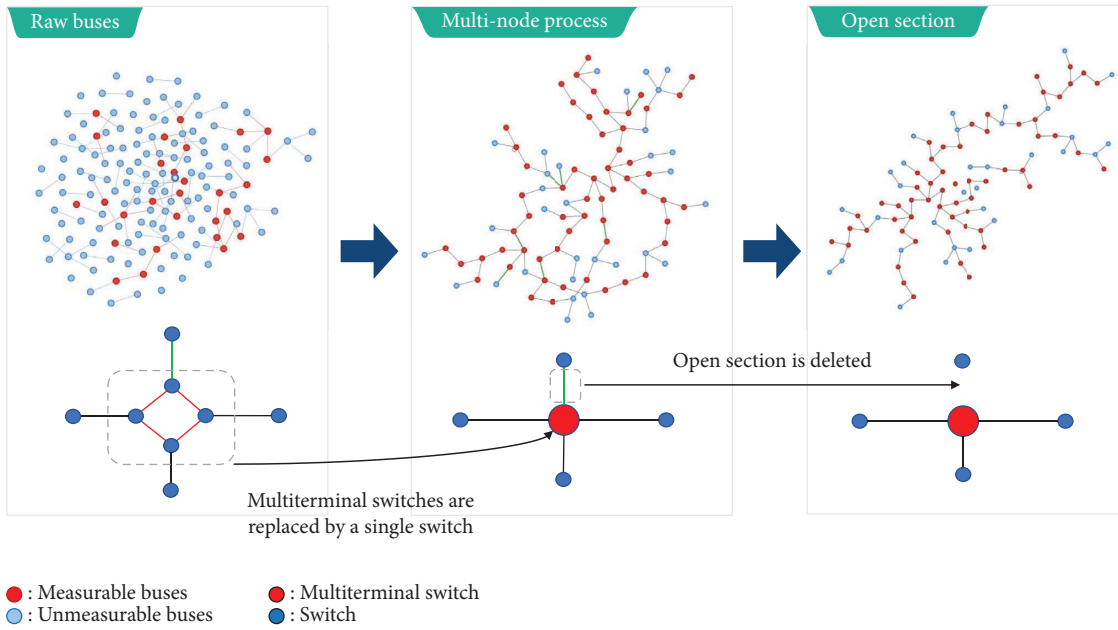

Figure 6: Schematic of a network topology change made using the PreprocessTopology function.

4. Congestion Management

The congestion management techniques are conventionally developed for the transmission networks [22, 23] and also practically applied to the transmission networks. The techniques are recently developed for the distribution networks [20, 21, 24–28], but none of them is applied to the real distribution networks. This section is dedicated to elaborate the implementation of the distribution network congestion management algorithm considering preprocessed data from the real distribution network DB rather than the development of new methodologies.

The data tables shown in Figure 7 are used for power flow calculation by the relevant module, which returns the results PF^{g}, Jacobian matrices $\mathbf{J}^{\mathrm{B}}$ with respect to bus injection powers and $\mathbf{J}^{\mathrm{L}}$ with respect to line flows, and DER

```
Input: B^0, L^0, PMS, J, L^open
Output: Updated B^0, L^0
for each line in L^0
    if line.From is not a bus and belongs to a different line's To then
        add line into tempLineFrom
    if line.To is not a bus then
        add line into tempLineTo
tempLine = merge tempLineFrom, tempLineTo
for each line in tempLine:
    delete line from L^0
    create a new line row
    combine each two From or To line info as a single line
for each CN_n in J: ◄ junction point generation
    add CN_n into B^0
for each bus in B^0:
    if bus is unusable or open:
        delete bus & delete line connected with bus
```

Algorithm 2: PreprocessTopology.

```
Input: L^0, c, count ⟵ 0
Output: L^0
if count ≥ |L^0| then
    print ("Exceed max iteration")
count ⟵ count + 1
if L_cn is empty then
    return
else then
    for n in L_cn do
        for d in L_nd do
            temp ⟵ b_lfd
    b_lfd ⟵ b_ltd
            b_ltd ⟵ temp
    for n in L_cn do
        MakeRadial (L^0, n, count)
end
```

Algorithm 3: MakeRadial.

operation status $\mathbf{O}^{\mathrm{D}}$. These data are input to the "GridConstraintSolution" function; the pseudocode is shown in Algorithm 5, where $\mathbf{P}^{\mathrm{L}}$ represents the power flows in all line sections, $\mathbf{P}^{\mathrm{D}}$ represents the injection powers from the DERs, $\mathbf{V}^{\mathrm{B}}$ denotes the voltage magnitudes at each bus, PC^{L} and VC^{B} are the line power flows and bus voltage magnitudes that violate the constraints, respectively, $\overline{P}$ and $\overline{V}/\underline{V}$ are the upper limit of the line power flow and upper/lower limits of the bus voltages, respectively, and $PC^{\mathrm{L,max}}$ and $VC^{\mathrm{B,max}}/VC^{\mathrm{B,min}}$ are the maximum violated line power flow and maximum/minimum violated bus voltages, respectively.

The "GridConstraintSolution" function checks for congestion by reviewing the power flow calculation result PF^{g}. If congestion is present, the algorithm finds the line and/or bus that violates the constraints most severely. Then, the output adjustments required for the DERs of $\mathbf{C}^{\mathrm{D}}$ that solve the congestion are calculated using Jacobian matrices $\mathbf{J}^{\mathrm{B}}$ and $\mathbf{J}^{\mathrm{L}}$. $\mathbf{J}^{\mathrm{B}}$ contains the first partial derivatives of the bus active and reactive powers according to the voltage magnitudes and angles [29], and $\mathbf{J}^{\mathrm{L}}$ contains the first partial derivatives of the line active and reactive power flows according to the voltage magnitudes and angles [30]. The parameters used to calculate $\mathbf{J}^{\mathrm{B}}$ and $\mathbf{J}^{\mathrm{L}}$ are fetched from $\mathbf{B}^{g}$ and $\mathbf{L}^{g}$, which are shown in Appendix. Matrix $\mathbf{J}^{\mathrm{B}}$ is related to the bus voltage and bus injection power as follows:

$$\Delta\mathbf{P}^{\mathrm{B}} = \mathbf{J}^{\mathrm{B}}\begin{bmatrix}\Delta\theta^{\mathrm{B}}\\ \Delta\mathbf{V}^{\mathrm{B}}\end{bmatrix}, \tag{1}$$

Input: $\mathbf{B^0}$, $\mathbf{L^0}$
Output: Updated $\mathbf{B^0}$, $\mathbf{L^0}$
1. $l_c \longleftarrow l_s$, $\mathbf{B^0} \longleftarrow \mathbf{B}^m \cup \mathbf{B}^j$
2. Stack.push(c)
3. while ($N_{\text{queue}} > 0$) do
4. $c \longleftarrow$Stack[end]
5. if b_{lfc} is not in $\mathbf{B^0}$ then
6. $l_c \longleftarrow l_p$ and l_c are combined as a single line
7. if $\mathbf{L}_{cn}$ is empty then
8. Stack.pop()
9. if b_{ltc} is not in $\mathbf{B}^{\text{m}}$ then
10. delete(b_{ltc}) in $\mathbf{B^0}$ & delete(l_c) in $\mathbf{L^0}$
11. [Stack.push(p) if b_{lfc} in $\mathbf{B}^j$]
12. else then
13. [Stack.pop() if b_{ltc} in $\mathbf{B^0}$]
14. [Stack.push(n) for n in $\mathbf{L}_{cn}$ if n is not in $\mathcal{Q}$]
15. End

Algorithm 4: ReduceMeteredOnlyTopology.

Table 2: Data structure of bus configuration $\mathbf{B}^g$.

Name of data	Meaning	Data type
Index	Index number of the bus	Integer
CEQID	ID number of the equipment at the bus	Integer
Name	Name of the bus	String
TYPE	Switch type in ID number	Integer
TYPEName	Name of switch type	String
ter1	ID number of one end of the bus	Integer
ter2	ID number of the other end of the bus	Integer
busType	Type of the bus (PQ, PV, and Slack)	Integer
VM	Voltage magnitude	Double
PG	Active power injection	Double
QG	Reactive power injection	Double
PL	Active power absorption	Double
QL	Reactive power absorption	Double
Pmeasure	Measured active power	Double
Qmeasure	Measured reactive power	Double
Vtheta	Voltage angle	Double

Table 3: Data structure of line configuration $\mathbf{L}^g$.

Name of data	Meaning	Data type
Index	Index number of the line	Integer
From	Bus number at the end of the line	Integer
To	Bus number at the other end of the line	Integer
Resistance	Line resistance	Double
Reactance	Line reactance	Double
ParentCEQID	ID number of the equipment at the end of the line	Integer
ChildCEQID	ID number of the equipment at the other end of the line	Integer
lineCurrentLimit	Ampacity of the line	Integer

Table 4: Data structure of DER configuration $\mathbf{D}^g$.

Name of data	Meaning	Data type
Index	Index number of the DER	Integer
GENID	ID number of the generator	Integer
Name	Name of the DER	
CEQFK	CEQID of the DER	Integer
DerCode	ID number of the DER	Integer
CenterCode	Center (subset of a head office) code to which the DER belongs	Integer
HeadOfficeCode	Head office code to which the DER belongs	Integer
HeadOfficeName	Head office name to which the DER belongs	
OfficeCode	Office (subset of a center) code to which the DER belongs	Integer
StationCode	Substation code to which the DER belongs	Integer
StationName	Substation name to which the DER belongs	
DLID	DL code to which the DER belongs	Integer
DLName	DL name to which the DER belongs	
generatorType	Generator type code	Integer
IsVirtualDER	Check whether the DER is virtual	Integer (binary)
TypeName	Generator type	
RTUMapID	RTU mapping ID	Integer
RUID	RU ID	Integer
LinkEquipment	SMGW equipment number to which the DER is connected	Integer
Cvppfk	CVPP ID to which the DER is connected	Integer
cvppCode	CVPP code to which the DER is connected	Integer
cvppName	CVPP name to which the DER is connected	Integer
tInstalled	Installation date	Integer
Capacity	Capacity	Double
maxLeadingReactivePower	Maximum reactive power for leading power factor	Double
maxLaggingReactivePower	Maximum reactive power for lagging power factor	Double
controllablePowerFactor	Power factor controllable range	Double
Efficiency	Efficiency	Double
storageCapacity	Storage capacity for ESS	Double
PG	Active power generation	Double
QG	Reactive power generation	Double
derAvailable	DER operation status	Integer (binary)
activePowerControllable	Active power control availability	Integer
upwardControlAmoun	Active power increases available amount	Double
downwardControlAmoun	Active power decreases available amount	Double
essNowEnergyAmount	ESS current storage energy	Double
essMaxAvailableEnergy	ESS maximum output	Double
essMinAvailableEnergy	ESS maximum charge	Double

where

$$\mathbf{J}^{\mathrm{B}} := \begin{bmatrix} \mathbf{J}_{\mathrm{P}\theta} & \mathbf{J}_{\mathrm{PV}} \\ \mathbf{J}_{\mathrm{Q}\theta} & \mathbf{J}_{\mathrm{QV}} \end{bmatrix}, \tag{2}$$

$$\begin{aligned} \mathbf{J}_{P\theta} &= \begin{bmatrix} \frac{\partial P_2}{\partial \theta_2} & \cdots & \frac{\partial P_2}{\partial \theta_n} \\ \vdots & \ddots & \vdots \\ \frac{\partial P_n}{\partial \theta_2} & \cdots & \frac{\partial P_n}{\partial \theta_n} \end{bmatrix}, \\ \mathbf{J}_{PV} &= \begin{bmatrix} \frac{\partial P_2}{\partial |V_2|} & \cdots & \frac{\partial P_2}{\partial |V_n|} \\ \vdots & \ddots & \vdots \\ \frac{\partial P_n}{\partial |V_2|} & \cdots & \frac{\partial P_n}{\partial |V_n|} \end{bmatrix}, \\ \mathbf{J}_{Q\theta} &= \begin{bmatrix} \frac{\partial Q_2}{\partial \theta_2} & \cdots & \frac{\partial Q_2}{\partial \theta_n} \\ \vdots & \ddots & \vdots \\ \frac{\partial Q_n}{\partial \theta_2} & \cdots & \frac{\partial Q_n}{\partial \theta_n} \end{bmatrix}, \\ \mathbf{J}_{QV} &= \begin{bmatrix} \frac{\partial Q_2}{\partial |V_2|} & \cdots & \frac{\partial Q_2}{\partial |V_n|} \\ \vdots & \ddots & \vdots \\ \frac{\partial Q_n}{\partial |V_2|} & \cdots & \frac{\partial Q_n}{\partial |V_n|} \end{bmatrix}, \end{aligned} \tag{3}$$

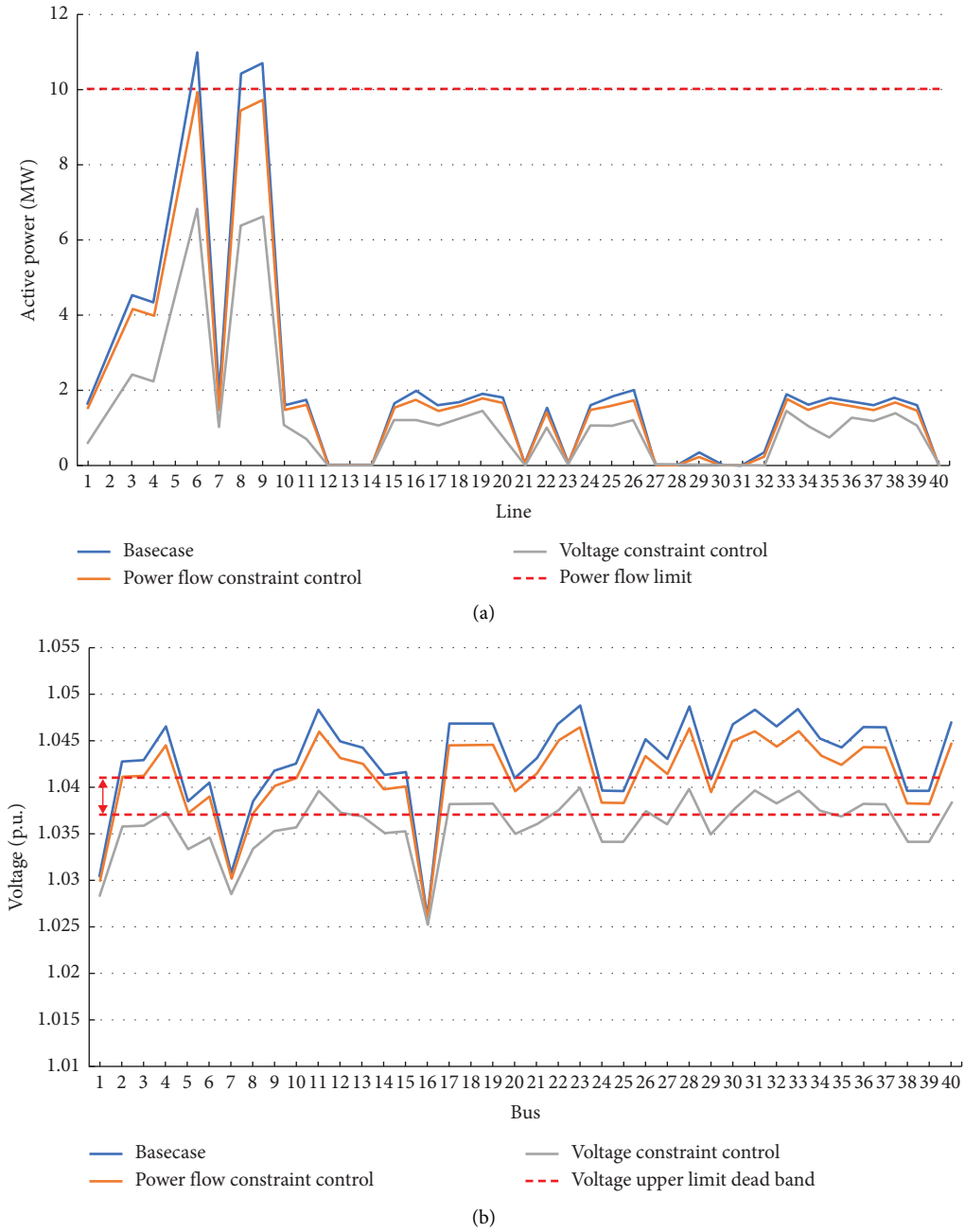

Figure 7: Network constraint limits and solutions for (a) line power flows and (b) bus voltages.

Input: PF^{g}, $\mathbf{J}^{\mathrm{B}}$, $\mathbf{J}^{\mathrm{L}}$, $\mathbf{O}^{\mathrm{D}}$
Output: CV^{g}, $\mathrm{PF}^{\mathrm{g}*}$, $\mathbf{C}^{\mathrm{D}}$
1. Get $\mathbf{P}^{\mathrm{L}}$ from (PF^{g})
2. if ($\max(\mathbf{P}^{\mathrm{L}}) > \overline{P}$) then
3. Get PC^{L}, $PC^{\mathrm{L,max}}$ from (PF^{g})
4. while ($PC^{\mathrm{L,max}} \leq \overline{P}$) do
5. Get $\mathbf{P}^{\mathrm{D}}$ from ($\mathbf{O}^{\mathrm{D}}$)
6. Compute $\mathbf{C}^{\mathrm{D}}$ from (PF^{g}, $\mathbf{J}^{\mathrm{B}}$, $\mathbf{J}^{\mathrm{L}}$, $\mathbf{O}^{\mathrm{D}}$)
7. $\mathbf{P}^{\mathrm{D}} \longleftarrow \mathbf{P}^{\mathrm{D}} - \mathbf{C}^{\mathrm{D}}$
8. Update PF^{g}, $\mathbf{J}^{\mathrm{B}}$, $\mathbf{J}^{\mathrm{L}}$, $\mathbf{O}^{\mathrm{D}}$ by running the Power Flow Algorithm
9. Update PC^{L}, $PC^{\mathrm{L,max}}$ from (PF^{g})
10. end
11. Get $\mathbf{V}^{\mathrm{B}}$ from (PF^{g})
12. if ($\max(\mathbf{V}^{\mathrm{B}}) > \overline{V}$) then
13. Get VC^{B}, $VC^{\mathrm{B,max}}$ from (PF^{g})
14. while ($VC^{\mathrm{B,max}} \leq \overline{V}$) do
15. Get $\mathbf{P}^{\mathrm{D}}$ from ($\mathbf{O}^{\mathrm{D}}$)
16. Compute $\mathbf{C}^{\mathrm{D}}$ from (PF^{g}, $\mathbf{J}^{\mathrm{B}}$, $\mathbf{O}^{\mathrm{D}}$)
17. $\mathbf{P}^{\mathrm{D}} \longleftarrow \mathbf{P}^{\mathrm{D}} + \mathbf{C}^{\mathrm{D}}$
18. Update PF^{g}, $\mathbf{J}^{\mathrm{B}}$, $\mathbf{O}^{\mathrm{D}}$ by running the Power Flow Algorithm
19. Update VC^{B}, $VC^{\mathrm{B,max}}$ from (PF^{g})
20. else if ($\min(\mathbf{V}^{\mathrm{B}}) < \underline{V}$) then
21. Get VC^{B}, $VC^{\mathrm{B,min}}$ from (PF^{g})
22. while ($VC^{\mathrm{B,min}} \geq \underline{V}$) do
23. Get $\mathbf{P}^{\mathrm{D}}$ from ($\mathbf{O}^{\mathrm{D}}$)
24. Compute $\mathbf{C}^{\mathrm{D}}$ from (PF^{g}, $\mathbf{J}^{\mathrm{B}}$, $\mathbf{O}^{\mathrm{D}}$)
25. $\mathbf{P}^{\mathrm{D}} \longleftarrow \mathbf{P}^{\mathrm{D}} + \mathbf{C}^{\mathrm{D}}$
26. Update PF^{g}, $\mathbf{J}^{\mathrm{B}}$, $\mathbf{O}^{\mathrm{D}}$ by running the Power Flow Algorithm
27. Update VC^{B}, $VC^{\mathrm{B,min}}$ from (PF^{g})
28. end

Algorithm 5: GridConstraintSolution.

$$\frac{\partial P_i}{\partial \theta_k} = \begin{cases} |V_i||V_k|\left(G_{ik}\sin\theta_{ik} - B_{ik}\cos\theta_{ik}\right), & i \neq k, \\ -Q_i - B_{ii}|V_i|^2, & i = k, \end{cases}$$

$$\frac{\partial P_i}{\partial |V_{k|}} = \begin{cases} |V_i|\left(G_{ik}\cos\theta_{ik} + B_{ik}\sin\theta_{ik}\right), & i \neq k, \\ \dfrac{P_i}{|V_i|} + G_{ii}|V_i|, & i = k, \end{cases}$$

$$\frac{\partial Q_i}{\partial \theta_k} = \begin{cases} -|V_i||V_k|\left(G_{ik}\cos\theta_{ik} + B_{ik}\sin\theta_{ik}\right), & i \neq k, \\ P_i - G_{ii}|V_i|^2, & i = k, \end{cases}$$

$$\frac{\partial Q_i}{\partial |V_k|} = \begin{cases} |V_i|\left(G_{ik}\sin\theta_{ik} - B_{ik}\cos\theta_{ik}\right), & i \neq k, \\ \dfrac{Q_i}{|V_i|} - B_{ii}|V_i|, & i = k, \end{cases} \tag{4}$$

where G_{ik} and G_{ik} are conductance and susceptance between nodes i and k, respectively, θ_{ik} is the voltage angle difference between nodes i and k, and θ^{B} is the bus voltage angle. From (1), it is possible to determine the extent to which the outputs of DERs ($\Delta\mathbf{P}^{\mathrm{D}}$, where $\Delta\mathbf{P}^{\mathrm{D}} \subset \Delta\mathbf{P}^{\mathrm{B}}$) should be adjusted to solve the bus voltage violation ($\Delta\mathbf{V}^{\mathrm{B}}$). The sensitivity of the i th bus injection power to the j th bus voltage is equivalent to the element in the i th row and $N^{\mathrm{B}} + j$ th column of $\mathbf{J}^{\mathrm{B}}$, where N^{B} is the number of buses. The matrix $\mathbf{J}^{\mathrm{L}}$ is related to the bus injection power and line power flow as follows [30]:

$$\Delta\mathbf{P}^{\mathrm{B}} = \mathbf{J}^{\mathrm{B}}\left(\mathbf{J}^{\mathrm{L}}\right)^{-1}\Delta\mathbf{P}^{\mathrm{L}}, \tag{5}$$

where

$$\mathbf{J}^{\mathrm{L}} \coloneqq \begin{bmatrix} \mathbf{J}_{\mathrm{P}'\theta} & \mathbf{J}_{\mathrm{P}'\mathrm{V}} \\ \mathbf{J}_{\mathrm{Q}'\theta} & \mathbf{J}_{\mathrm{Q}'\mathrm{V}} \end{bmatrix}, \tag{6}$$

$$\begin{aligned}
\mathbf{J}_{P'\theta} &= \begin{bmatrix} \frac{\partial P_{1,2}}{\partial \theta_2} & \cdots & \frac{\partial P_{1,2}}{\partial \theta_n} \\ \vdots & \ddots & \vdots \\ \frac{\partial P_{n-1,n}}{\partial \theta_2} & \cdots & \frac{\partial P_{n-1,n}}{\partial \theta_n} \end{bmatrix}, \\
\mathbf{J}_{P'V} &= \begin{bmatrix} \frac{\partial P_{1,2}}{\partial |V_2|} & \cdots & \frac{\partial P_{1,2}}{\partial |V_n|} \\ \vdots & \ddots & \vdots \\ \frac{\partial P_{n-1,n}}{\partial |V_2|} & \cdots & \frac{\partial P_{n-1,n}}{\partial |V_n|} \end{bmatrix}, \\
\mathbf{J}_{Q'\theta} &= \begin{bmatrix} \frac{\partial Q_{1,2}}{\partial \theta_2} & \cdots & \frac{\partial Q_{1,2}}{\partial \theta_n} \\ \vdots & \ddots & \vdots \\ \frac{\partial Q_{n-1,n}}{\partial \theta_2} & \cdots & \frac{\partial Q_{n-1,n}}{\partial \theta_n} \end{bmatrix}, \\
\mathbf{J}_{Q'V} &= \begin{bmatrix} \frac{\partial Q_{1,2}}{\partial |V_2|} & \cdots & \frac{\partial Q_{1,2}}{\partial |V_n|} \\ \vdots & \ddots & \vdots \\ \frac{\partial Q_{n-1,n}}{\partial |V_2|} & \cdots & \frac{\partial Q_{n-1,n}}{\partial |V_n|} \end{bmatrix},
\end{aligned} \tag{7}$$

$$\begin{aligned}
\frac{\partial P_{i,k}}{\partial \theta_m} &= \begin{cases} |V_i||V_k|(G_{ik}\sin\theta_{ik} - B_{ik}\cos\theta_{ik}), & m = i, \\ -|V_i||V_k|(G_{ik}\sin\theta_{ik} - B_{ik}\cos\theta_{ik}), & m = k, \\ 0, & \text{otherwise}, \end{cases} \\
\frac{\partial P_{i,k}}{\partial |V_m|} &= \begin{cases} 2|V_i|G_{ik} - |V_k|(G_{ik}\cos\theta_{ik} + B_{ik}\cos\theta_{ik}), & m = i, \\ -|V_i|(G_{ik}\cos\theta_{ik} + B_{ik}\sin\theta_{ik}), & m = k, \\ 0, & \text{otherwise}, \end{cases} \\
\frac{\partial Q_{i,k}}{\partial \theta_m} &= \begin{cases} -|V_i||V_k|(G_{ik}\cos\theta_{ik} + B_{ik}\sin\theta_{ik}), & m = i, \\ |V_i||V_k|(G_{ik}\cos\theta_{ik} + B_{ik}\sin\theta_{ik}), & m = k, \\ 0, & \text{otherwise}, \end{cases} \\
\frac{\partial Q_{i,k}}{\partial |V_m|} &= \begin{cases} -2|V_i|(B_{i0} + B) - |V_k|(G_{ik}\sin\theta_{ik} - B_{ik}\cos\theta_{ik}), & m = i, \\ -|V_i|(G_{ik}\sin\theta_{ik} - B_{ik}\cos\theta_{ik}), & m = k, \\ 0, & \text{otherwise}, \end{cases}
\end{aligned} \tag{8}$$

where $P_{i,k}$ is power flow from node i to k. From (5), it is possible to determine the extent to which the outputs of DERs ($\Delta\mathbf{P}^{\mathrm{D}}$) should be adjusted to solve a line capacity violation ($\Delta\mathbf{P}^{\mathrm{L}}$). The sensitivity of the i th bus injection power to the j th line power flow is equivalent to the element in the i th row and j th column of $\mathbf{J}^{\mathrm{B}}(\mathbf{J}^{\mathrm{L}})^{-1}$. The sensitivities of DER-connected buses must be readjusted as follows:

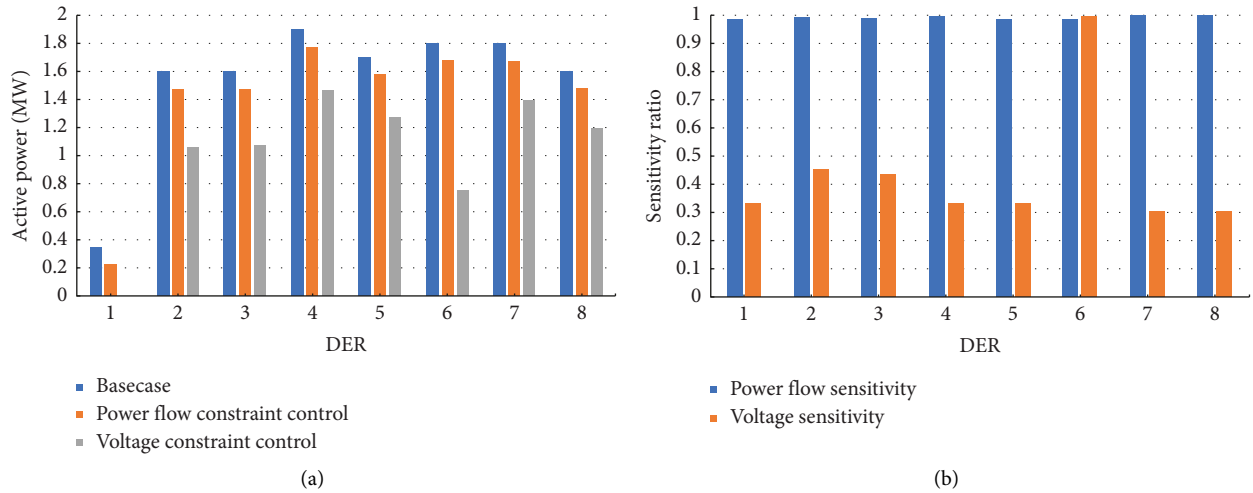

Figure 8: DER (a) outputs and (b) sensitivity ratios.

$$\xi_i = \frac{\partial P_i^{\mathrm{D}} / \partial CV^{\mathrm{g,max}}}{\sum_{i=1}^{N^{\mathrm{D}}} \partial P_i^{\mathrm{D}} / \partial CV^{\mathrm{g,max}}}, \tag{9}$$

where N^{D} is the number of DERs, $CV^{\mathrm{g,max}}$ is the maximum CV^{g} (the combined matrix of PC^{L} and VC^{B}), and P_i^{D} is the i th element of $\mathbf{P}^{\mathrm{D}}$:

$$\sum_{i=1}^{N^{\mathrm{D}}} \xi_i = 1. \tag{10}$$

Ultimately, the i th DER output power adjustment (the i th element of $\mathbf{C}^{\mathrm{D}}$, i.e., C_i^{D}) is calculated as follows:

$$C_i^{\mathrm{D}} = \xi_i \times CV^{\mathrm{g,max}}. \tag{11}$$

5. Simulations

The real-time DMS algorithm was applied to a real DL of KEPCO, i.e., the Sandan DL in Gwangju, South Korea. The nominal voltage of the network is 22.9 kV. The network topology of the Sandan DL was derived by the topology configuration module. Although congestion of the real distribution network is impossible given the regulations and grid requirements, the utility of our congestion management system was indirectly proven by applying the algorithm to a semireal distribution network environment, i.e., a real network DB combined with measurements from vDER emulators. In other words, the voltage and line capacity violation cases are made up, and the temporal pattern of power flow is not considered. The type of DERs is not considered since the generation pattern and control dynamics are not critical issues in this study. When extra power was injected by the vDERs, line flow and bus voltage constraint violations were simulated. Accuracy was tested by comparing the real measurement data to the outputs of the power flow calculation module.

The algorithm solved the congestions, as shown in Figure 7. For each line, Figure 7(a) shows the active power line flow limits, base case power flows, adjusted power flows that solve line congestion, and adjusted power flows that solve bus voltage violations. With the base scenario (blue line), it can be seen that the active power exceeds its limit at lines 6, 8, and 9. After being adjusted by the developed algorithm (orange line), the power flow could be adjusted such that it was just below the limit at line 6 since line 6 was the most congested line. By solving the congestion at line 6, the other congested lines (lines 8 and 9) are solved subordinately. However, the voltage violation cannot be solved by solving the line capacity limitation as shown in Figure 7(b). For each bus, Figure 7(b) shows the voltage upper limit dead band, base case bus voltages, adjusted voltages that solve line congestion, and adjusted voltages that solve bus voltage violation. The voltage dead band is set to prevent frequent operation of power adjustment while the voltage is fluctuating around the upper limit, which is 1.039 pu in South Korea [1]. The dead band is set as ± 0.002 pu here, which results the dead band of 1.037–1.041 pu of voltage upper limit. So, if the voltage at every bus is adjusted below 1.041 pu, the algorithm stops. As shown in the figure, the voltages at many buses are still violated even after the power adjustment to solve the line congestion (orange line). In such a case, the power flow must be further adjusted based on voltage sensitivity. And by doing so, it shows that the voltage violation can be solved (gray line). Note that solving voltage violation further drops the line power flows as shown in Figure 7(a) (gray line).

Figure 8 shows the active output powers of DERs and DER sensitivity ratios. Figure 8(a) shows that to solve line congestion problem, the DERs lower their output power than those of the base case. In order to solve voltage violation problem, they lower the output power further. Figure 8(b) shows two sensitivities—the line power flow to DER output sensitivity and the voltage to DER output sensitivity. The sensitivity values are normalized for each sensitivity type, and their maximum value is 1. Note that the line power flow sensitivities have almost the same values with each other. Hence, they reduce almost the same output power to solve line congestion problem as shown in Figure 8(a)—It shows

Table 5: Power curtailment of DERs due to constraints.

DER number	Power flow constraint control (MW)	Voltage constraint control (MW)
1	−0.126759839	−0.348912
2	−0.126759839	−0.544168656
3	−0.126759839	−0.530718551
4	−0.126759839	−0.434801883
5	−0.126759839	−0.432759117
6	−0.126759839	−1.052274981
7	−0.126759839	−0.40764228
8	−0.126759839	−0.407644205
Sum	−1.014078713	−4.158921673

that the reduction rate from blue bar to orange bar is almost the same for all DERs. On the other hand, the voltage sensitivity values are significantly different from each other DER. So, while solving the voltage violation problem, DER 6 reduces much more output power than the others since it has a relatively large sensitivity value than the others. The comparison of Figures 8(a) and 8(b) shows that the DER output powers are proportional to the sensitivity ratios. The exact amount of power curtailed from the base case scenario is shown in Table 5. It is shown that the power is evenly curtailed for the case of power flow constraint control whereas the amount of the curtailment varies for the case of voltage constraint control. This result matches with the sensitivity result as shown in Figure 8(b).

6. Future Works and Conclusions

This paper is dedicated to (1) explain the features and data of the South Korean distribution network, (2) illustrate practical obstacles encountered during distribution network analysis, (3) apply real data of the distribution network for network congestion management by controlling DERs, and (4) introduce expected future problems while deploying DSO functions in the distribution network. During the development of a DMS algorithm for a real distribution network, many gaps between theory and practice have been found. For example, the DB lacks "load buses" for power flow calculation, and many nodes are unnecessary from the perspective of network analysis. In other words, the DB was constructed for asset management rather than network analysis. Several problems have been solved, as described herein, but many remain as follows:

- The data sampling rate: The FRTUs of the distribution network send data to the DMS every 15 min. As many DERs in the network exhibit large power fluctuations within 15 min (e.g., PVs and EVs), a more granular sampling rate is required for true real-time DMS.
- Phase identification: The phases of the line sections do not match. Measurement devices were randomly installed in terms of phase; it is almost impossible to derive distribution networks for each phase. Given this load imbalance, phase identification techniques are required for more precise congestion management.
- Voltage measurement error: This error is very large given the physical limitations of overhead lines [31], and the measurements cannot be used for optimal management. The measurement environment of the distribution network is highly restrictive. For optimal management of a distribution network with high DER penetration, a practical state estimation method that considers the real distribution network environment, or cheap but accurate measurement devices, is required.
- Topological change: Frequent topological changes in a distribution network pose well-documented problems. Many researchers have studied this, but it is worth mentioning again here because it significantly affects network analysis. Given the power fluctuations of DERs in a distribution network, much faster and more frequent topology identification techniques are required.
- DB structure: Academics seldom have access to the raw data for an entire distribution network. It is found that the raw data were structured to aid asset management by field engineers. A large proportion of the data are unnecessary for network analysis; fewer data would aid real-time network management. As DSOs are becoming essential as DERs penetrate further, many parts of the DB should be restructured with consideration of the needs of field engineers and managers.

The simulation results (Figures 7 and 8) are also significantly noteworthy in terms of the CVPP business in South Korea since the reduction of the output power means the decrement of the CVPP owner's profit. As shown in Figure 8(b), the location (bus) of the DER affects the reduction rate of the output power a lot. It could make the CVPP owners avoid certain locations (buses) in the distribution network if the output power reduction is conducted based on the sensitivity analysis without providing any compensation for the power reduction. The development of the business model for the CVPP is still an ongoing debate in Korea so these results could be referred to the parties who develops and legislates the business model.

The DSO concept is relatively new in South Korea, and many gaps between theoretical and real distribution network environments have been found during the development of a DSO for the South Korean distribution network. Our goal is precise per-phase congestion management of a distribution network with a DER control frequency of < 5 min. This paper describes our efforts and work to date. It is expected that more academics and engineers will be inspired to solve the practical problems of the Korean distribution network. In particular, an efficient DSO is urgently required.

Nomenclature

Acronym

CEQ	Conducting equipment
CN	Connectivity node
CVPP	Commercial virtual power plant
DB	Database
DER	Distributed energy resource
DERMS	Distributed energy resource management system
DL	Distribution line
DMS	Distribution management system
DNO	Distribution network owner

DSO	Distribution system operator
EV	Electric vehicle
FRTU	Feeder remote terminal unit
ID	Identification
KDERMS	Korean DERMS
KEPCO	Korean electric power corporation
KPX	Korean power exchange
KSDMS	Korean smart distribution management system
PMS	Pad-mounted switch
pu	Per unit
PV	Photovoltaic
RES	Renewable energy source
SMGW	Smart gateway
T	Terminal
TSO	Transmission system operator
vDER	Virtual DER

Names of Algorithm Function and Their Purposes

readUserInfo	Reads user information
connectPythontoSql	Accesses the DB via Python code
importSql	Imports data from the DB
ComposeTopology	Returns lists of the types of switches and CNs
PreprocessTopology	Returns the initial reduced bus and line data tables
MakeRadial	Reduces the network topology
ReduceMeteredOnlyTopology	Further reduces the network topology by eliminating unmeasurable buses
ImportMeteredData	Import the measured data from the DB
GridConstraintSolution	Checks for congestion

Datasets in a Matrix Notation

$\mathbf{M}^{rD}/\mathbf{M}^{vD}$	Measurements from the DERs/vDERs
$\mathbf{M}^{D}$	Measurements from both the DERs and vDERs
$\mathbf{M}^{F}$	Measurements from the FRTUs
$\mathbf{G}^{g}$	Information from the grid
$\mathbf{O}^{D}$	Operational information of the DERs
$\mathbf{C}^{D}$	Power curtailment required for each DER
$\mathbf{B}^{g}/\mathbf{L}^{g}/\mathbf{D}^{g}$	Configuration datasets of the bus/line/DER
$\mathbf{B}^{0}/\mathbf{L}^{0}$	Initial reduced bus/line data tables
$\mathbf{B}^{m}/\mathbf{B}^{j}$	Measurement/junction buses
PF^{g}/PF^{g*}	Power flow calculation results before/after handling the violations
$\mathbf{J}^{B}/\mathbf{J}^{L}$	Jacobian matrices with respect to the bus injection power/the line flows
PC^{L}/ VC^{B}	Line power flows/bus voltage magnitudes that violate the constraints
CV^{g}	Constraint violations (combined dataset of PC^{L} and VC^{B})
$\mathbf{P}^{L}$	Power flows in all line sections
$\mathbf{P}^{D}/\mathbf{P}^{B}$	Injection powers from the DERs/buses
$\mathbf{V}^{B}/\theta^{B}$	Voltage magnitudes/angles at each bus

Indices

Some indices are used and represented as subscripts and described in the body of the paper

Appendix

The line and bus data used for the power flow calculation in this study are shown in Tables A1 and A2. These are part of $\mathbf{B}^{g}$ and $\mathbf{L}^{g}$. "Slack," "PV," and "PQ" buses are denoted as 1, 2, and 3, respectively, for "busType" in Table A1. For "resistance" and "reactance" in Table A2, pu is used for the unit and the base power and voltage are 1 MVA and 22.9 kV, respectively.

Table A1: Part of bus data from $\mathbf{B}^{g}$.

Index	busType	PL (MW)	QL (MW)
1	3	0	0
2	3	−0.020091858	0.202290882
3	3	0.354283417	−0.120149799
4	3	0.355876801	−0.101054077
5	3	0.160405960	0.049962753
6	3	0.182191406	0.209318217
7	3	1.124598877	−0.082120789
8	3	0.25890596	−0.024037247
9	3	0.151191406	0.008818217
10	3	0.171192383	0.633060005
11	3	−0.612000000	−0.104000000
12	3	0.362238037	0.244274261
13	3	0.569428894	0.621447662
14	3	0.957079163	0.129027644
15	3	0.176387756	0.050709427
16	1	1.039598877	0.226879211
17	3	0	0
18	3	0	0
19	3	0	0
20	3	0	0
21	3	0	0
22	3	0	0
23	3	0	0
24	3	0	0
25	3	0	0
26	3	0	0
27	3	0	0
28	3	0	0
29	3	0	0
30	3	0	0
31	3	0	0
32	3	0	0
33	3	0	0
34	3	0	0
35	3	0	0
36	3	0	0
37	3	0	0
38	3	0	0
39	3	0	0
40	3	0	0

Table A2: Part of line data from $\mathbf{L}^g$.

Index	From	To	Resistance (pu)	Reactance (pu)
1	2	3	8.6E − 05	1.4E − 04
2	10	2	6.2E − 05	1.0E − 04
3	9	10	1.7E − 04	3.7E − 05
4	6	9	3.0E − 04	2.7E − 04
5	35	6	1.3E − 04	1.8E − 04
6	8	35	1.0E − 04	1.7E − 04
7	6	14	5.1E − 04	2.1E − 04
8	16	7	5.7E − 04	9.4E − 04
9	7	8	7.8E − 04	1.3E − 03
10	2	24	1.8E − 04	7.8E − 05
11	3	4	2.2E − 03	9.1E − 04
12	8	5	3.0E − 03	1.3E − 03
13	7	1	4.3E − 05	7.1E − 05
14	28	11	1.2E − 03	4.6E − 04
15	30	28	1.2E − 03	4.2E − 04
16	13	12	4.3E − 04	1.4E − 04
17	11	25	2.6E − 04	1.1E − 04
18	6	26	1.8E − 04	7.8E − 05
19	4	27	1.8E − 04	7.8E − 05
20	10	13	1.1E − 03	4.8E − 04
21	12	29	1.7E − 04	3.7E − 05
22	14	15	1.8E − 04	7.8E − 05
23	15	30	1.4E − 03	5.6E − 04
24	28	36	1.0E − 03	3.6E − 04
25	36	17	1.7E − 04	3.7E − 05
26	36	18	3.7E − 05	1.6E − 05
27	36	19	3.7E − 05	1.6E − 05
28	31	20	3.7E − 05	1.6E − 05
29	32	21	3.7E − 05	1.6E − 05
30	33	22	3.7E − 05	1.6E − 05
31	34	23	3.7E − 05	1.6E − 05
32	26	31	3.7E − 05	1.6E − 05
33	31	37	3.7E − 05	1.6E − 05
34	24	32	3.7E − 05	1.6E − 05
35	32	38	3.7E − 05	1.6E − 05
36	27	33	3.7E − 05	1.6E − 05
37	33	39	3.7E − 05	1.6E − 05
38	25	34	3.7E − 05	1.6E − 05
39	34	40	3.7E − 05	1.6E − 05

Data Availability Statement

The data presented in this study are available on request from the corresponding author. The data are not publicly available due to the KEPCO data management policy. Some available data are presented in the Appendix.

Disclosure

The authors would like to declare that a preprint of this paper has previously been published [32] though there are major revisions in this paper.

Conflicts of Interest

The authors declare no conflicts of interest.

Funding

This work was supported by the Korea Institute of Energy Technology Evaluation and Planning (KETEP) and the Ministry of Trade, Industry, & Energy (MOTIE) of the Republic of Korea (No. 20225500000060). This work was supported by the National Research Foundation of Korea (NRF) grant funded by the Korea Government the Ministry of Science and Information and Communication Technology (MSIT) (No. 2022R1C1C1008910).

Acknowledgments

This work was supported by the National Research Foundation of Korea (NRF) grant funded by the Korea Government the Ministry of Science and Information and Communication Technology (MSIT) (No. 2022R1C1C1008910) and the Korea Institute of Energy Technology Evaluation and Planning (KETEP) and the Ministry of Trade, Industry, & Energy (MOTIE) of the Republic of Korea (No. 20225500000060).

References

[1] KEPCO, *Terms of Use for Transmission and Distribution Electricity Equipment* (Jeollanamdo, South Korea: KEPCO. Naju, 2022), https://cyber.kepco.co.kr/ckepco/front/jsp/CY/H/C/CYHCHP00601.jsp.

[2] S. Cho, *Current Status and Prospect of Global Distribution Network Renewable Energy Flexible Interconnection* (Seoul, South Korea: Presented at CIRED Korean National Committee, 2022).

[3] Ministry of Trade Industry and Energy of South Korea, *The 10th Basic Plan for Electricity Supply and Demand* (Seoul, South Korea: Ministry of Trade, Industry, and Energy. Sejong, 2023), https://www.motie.go.kr/motie/ms/nt/announce3/bbs/bbsView.do?bbs_seq_n=68162&bbs_cd_n=6&currentPage=1&search_key_n=&cate_n=&dept_v=&search_val_v=&biz_anc_yn_c=.

[4] D. Apostolopoulou, S. Bahramirad, and A. Khodaei, "The Interface of Power: Moving toward Distribution System Operators," *IEEE Power and Energy Magazine* 14, no. 3 (2016): 46–51, https://doi.org/10.1109/MPE.2016.2524960.

[5] L. Strezoski, H. Padullaparti, F. Ding, and M. Baggu, "Integration of Utility Distributed Energy Resource Management System and Aggregators for Evolving Distribution System Operators," *Journal of Modern Power Systems and Clean Energy* 10, no. 2 (2022): 277–285, https://doi.org/10.35833/MPCE.2021.000667.

[6] Irena, *Innovation Landscape Brief*: *Future Role of Distribution System Operators* (Abu Dhabi, UAE: International Renewable Energy Agency, 2019).

[7] S. McCafferty, "Distribution System Operator (DSO) Models for Utility Stakeholders: Organizational Models for a Digital," *Distributed Modern Grid, Black & Veatch Management Consulting* (New York, NY: LLC, 2021).

[8] I.-K. Song, S.-Y. Yun, S.-C. Kwon, and N.-H. Kwak, "Design of Smart Distribution Management System for Obtaining Real-Time Security Analysis and Predictive Operation in Korea," *IEEE Transactions on Smart Grid* 4, no. 1 (2013): 375–382, https://doi.org/10.1109/TSG.2012.2233769.

[9] J. Hu, S. You, M. Lind, and J. Ostergaard, "Coordinated Charging of Electric Vehicles for Congestion Prevention in the Distribution Grid," *IEEE Transactions on Smart Grid* 5, no. 2 (2014): 703–711, https://doi.org/10.1109/TSG.2013.2279007.

[10] A. Picciariello, K. Alvehag, and L. Söder, "Impact of Network Regulation on the Incentive for DG Integration for the DSO: Opportunities for a Transition toward a Smart Grid," *IEEE*

Transactions on Smart Grid 6, no. 4 (July 2015): 1730–1739, https://doi.org/10.1109/TSG.2015.2409313.

[11] M. J. Dolan, E. M. Davidson, I. Kockar, G. W. Ault, and S. D. McArthur, "Distribution Power Flow Management Utilizing an Online Optimal Power Flow Technique," *IEEE Transactions on Power Systems* 27, no. 2 (May 2012): 790–799, https://doi.org/10.1109/tpwrs.2011.2177673.

[12] S. Huang and Q. Wu, "Dynamic Tariff-Subsidy Method for PV and V2G Congestion Management in Distribution Networks," *IEEE Transactions on Smart Grid* 10, no. 5 (2019): 5851–5860, https://doi.org/10.1109/TSG.2019.2892302.

[13] K. Oikonomou, M. Parvania, and R. Khatami, "Deliverable Energy Flexibility Scheduling for Active Distribution Networks," *IEEE Transactions on Smart Grid* 11, no. 1 (2020): 655–664, https://doi.org/10.1109/TSG.2019.2927604.

[14] S. Huang and Q. Wu, "Real-time Congestion Management in Distribution Networks by Flexible Demand Swap," *IEEE Transactions on Smart Grid* 9, no. 5 (2018): 4346–4355, https://doi.org/10.1109/TSG.2017.2655085.

[15] S. Huang, Q. Wu, H. Zhao, and C. Li, "Distributed Optimization-Based Dynamic Tariff for Congestion Management in Distribution Networks," *IEEE Transactions on Smart Grid* 10, no. 1 (2019): 184–192, https://doi.org/10.1109/TSG.2017.2735998.

[16] A. S. Bouhouras, N. S. Kelepouris, N. Koltsaklis, K. Oureilidis, and G. C. Christoforidis, "Congestion Management in Coupled TSO and DSO Networks," *Electric Power Systems Research* 229 (2024): 110145, https://doi.org/10.1016/j.epsr.2024.110145.

[17] F. García-Muñoz, A. Ivanova, J. Farré Montané, M. Serrano, and C. Corchero, "A DSO Flexibility Platform Based on an Optimal Congestion Management Model for the European CoordiNet Project," *Electric Power Systems Research* 221, no. 221 (2023): 109386, https://doi.org/10.1016/j.epsr.2023.109386.

[18] M. U. Hashmi, A. Koirala, H. Ergun, and D. Van Hertem, "Robust Flexibility Needs Assessment With Bid Matching Framework for Distribution Network Operators," *Sustainable Energy Grids and Networks* 34 (2023): 101069, https://doi.org/10.1016/j.segan.2023.101069.

[19] G. d. A. Terça, "Deliverable: D5.2 Methodology for Dynamic Distribution Grid Tariffs," *EUniversal Project Report* (Ch'ungch'ong-bukto, South Korea: UMEI, 2022), https://euniversal.eu/wp-content/uploads/2022/08/EUniversal_D5.2_Methodology-for-dynamic-distribution-grid-tariffs-.pdf.

[20] S. Huang, Q. Wu, S. S. Oren, R. Li, and Z. Liu, "Distribution Locational Marginal Pricing through Quadratic Programming for Congestion Management in Distribution Networks," *IEEE Transactions on Power Systems* 30, no. 4 (2015): 2170–2178, https://doi.org/10.1109/tpwrs.2014.2359977.

[21] O. G. M. Khan, A. Youssef, M. Salama, and E. El-Saadany, "Robust Multi-Objective Congestion Management in Distribution Network," *IEEE Transactions on Power Systems* 38, no. 4 (2023): 3568–3579.

[22] D. Shirmohammadi, B. Wollenberg, A. Vojdani, et al., "Transmission Dispatch and Congestion Management in the Emerging Energy Market Structures," *IEEE Transactions on Power Systems* 13, no. 4 (1998): 1466–1474, https://doi.org/10.1109/59.736292.

[23] R. S. Fang and A. K. David, "Transmission Congestion Management in an Electricity Market," *IEEE Transactions on Power Systems* 14, no. 3 (1999): 877–883, https://doi.org/10.1109/59.780898.

[24] S. Huang, Q. Wu, L. Cheng, Z. Liu, and H. Zhao, "Uncertainty Management of Dynamic Tariff Method for Congestion Management in Distribution Networks," *IEEE Transactions on Power Systems* 31, no. 6 (2016): 4340–4347, https://doi.org/10.1109/tpwrs.2016.2517645.

[25] S. Huang and Q. Wu, "Dynamic Subsidy Method for Congestion Management in Distribution Networks," *IEEE Transactions on Smart Grid* 9, no. 3 (2018): 2140–2151, https://doi.org/10.1109/tsg.2016.2607720.

[26] A. Asrari, M. Ansari, J. Khazaei, and P. Fajri, "A Market Framework for Decentralized Congestion Management in Smart Distribution Grids Considering Collaboration Among Electric Vehicle Aggregators," *IEEE Transactions on Smart Grid* 11, no. 2 (2020): 1147–1158, https://doi.org/10.1109/tsg.2019.2932695.

[27] J. Hu, J. Wu, X. Ai, and N. Liu, "Coordinated Energy Management of Prosumers in a Distribution System Considering Network Congestion," *IEEE Transactions on Smart Grid* 12, no. 1 (2021): 468–478, https://doi.org/10.1109/tsg.2020.3010260.

[28] M. Tofighi-Milani, S. Fattaheian-Dehkordi, M. Fotuhi-Firuzabad, and M. Lehtonen, "Decentralized Active Power Management in Multi-Agent Distribution Systems Considering Congestion Issue," *IEEE Transactions on Smart Grid* 13, no. 5 (2022): 3582–3593, https://doi.org/10.1109/tsg.2022.3172757.

[29] A. R. Bergen and V. Vittal, *Power Systems Analysis* (Upper Saddle River, NJ: Prentice Hall, 1999).

[30] I. Liere-Netheler, F. Schuldt, K. Maydell, and C. Agert, "Optimised Curtailment of Distributed Generators for the Provision of Congestion Management Services Considering Discrete Controllability," *IET Generation, Transmission & Distribution* 14, no. 5 (2020): 735–744, https://doi.org/10.1049/iet-gtd.2019.0992.

[31] S. Park and S. Lim, "Voltage Estimation Method for Distribution Line with Irregularly Dispersed Load," *The Transactions of the Korean Institute of Electrical Engineers* 67, no. 4 (2018): 491–497, https://doi.org/10.5370/KIEE.2018.67.4.491.

[32] J.-S. Park, J. H. Kim, S. G. Noh, et al., "Distribution System Operator (DSO) Functions in South Korea-Part I: Development, Practical Obstacles, and Future Work," *SSRN* (2023): https://doi.org/10.2139/ssrn.4435118.